# Location-specific weighting of the high-speed camera-based full-field model updating

**K. Zaletelj, J. Slavič, M. Boltežar**
University of Ljubljana, Faculty of mechanical engineering,
Aškerčeva 6, 1000 Ljubljana, Slovenia

## Abstract
Full-field modal shapes, identified from the high-speed camera measurement, offer local information of the structural behavior and have been successfully used to identify a large number of localized updating parameters. The camera based full-field shapes are typically contaminated with noise. In the finite element model updating procedure, the numerical response of the structure is compared with the measured data which are unreliable due to the noise and possibly lead to incorrect parameter identification. In this research, the local Signal-to-Noise Ratio (SNR) of the modal shape is investigated; two location specific weighting methods are implemented and their effect on model updating is evaluated. It was found that with the appropriate location-specific weights, the large number of localized parameters are successfully identified, and the localized anomalies of the structure are detected despite the noisy modal shapes.

## 1 Introduction

The field of finite-element-model updating is well established and is still in active development. Friswell *et al.* [1] researched finite-element-model updating in detail and classified it into the direct and sensitivity-based methods. Recently, Zhu *et al.* [2] proposed a substructure-based sensitivity method to accelerate the convergence of model updating. Rezaiee-Pajand *et al.* [3] presented an innovative, sensitivity-based updating strategy using a combination of the modal kinetic energy and the modal strain energy. Girardi *et al.* [4] proposed a numerical method for finding a global minimum of the cost function. Wan *et al.* [5] used a global-sensitivity analysis to decide on the best parameters to update.

High-speed imaging has become a popular approach for both static and dynamic measurements because it is a non-contact method and provides full-field response information. Lucas and Kanade [6] developed an algorithm for tracking a pattern as it moves across the camera's sensor. Peters *et al.* [7] used the approach in the field of mechanics, where it is known as Digital Image Correlation (DIC). The 3D response of the structure is identified using multiple synchronized high-speed cameras [8]; however, Gorjup *et al.* [9] showed that, using frequency-domain triangulation, the 3D operational shapes of a linear, time-invariant system can be identified using a single high-speed camera.

The use of high-speed-camera measurements in finite-element-model updating has the benefit of a large number of degrees of freedom being measured simultaneously, which enables the identification of local mode-shape features and the use of local correlation indicators. To achieve a spatial density of information similar to a high-speed camera by using accelerometers can be time consuming and a large number of sensors must be used, requiring sensors position optimization [10] and adding mass to the structure. One of the first uses of high-speed cameras for model updating was by Wang *et al.* [11] who used Tchebichef moment descriptors to describe modal shapes. Ngan *et al.* [12] used DIC measurements to investigate the Zernike moment descriptors. Zanarini [13] compared the updating results when the experimental data are obtained using high-speed cameras with 3D DIC algorithm, SLDV and ESPI. While Rohe *et al.* [14] successfully used SLDV measurements in the updating procedure, Zanarini showed that the 3D DIC and ESPI approaches were superior to SLDV. Recently, Cuadrado *et al.* [15] used the sensitivity approach to update the parameters of a composite plate using a full-field vibration measurement.

In this article, the use of three different weighting methods is researched and compared on a numerical case study. Full research is presented in a published article by Zaletelj et al. [16].

# 2 Theoretical background

A short summery of the displacement identification, modal identification and finite element model updating is given in this section.

## 2.1 Image-based displacement identification

A 2D digital image correlation (DIC) algorithm was used to identify the rigid translations of the selected subsets. Each subset provided information for a single measurement point. With DIC, the cost function is minimized, in our case:

$$S = \sum_x \sum_y \big(I_{\mathrm{ref}}(x,y) - I(x+\Delta x, y+\Delta y)\big)^2, \tag{1}$$

where $I_{\mathrm{ref}}$ represents the intensities of the subset of pixels on the reference image and $I$ on the current image. $\Delta x$ and $\Delta y$ represent the identified displacements of the subset on the current image with respect to the reference image in the horizontal and vertical directions, respectively.

## 2.2 Hybrid full-field experimental modal analysis

The Least-Squares Complex Frequency (LSCF) method [17] in combination with the Least-Squares Frequency Domain (LSFD) method [18, 19] was used in this research to identify the modal parameters from the identified displacements. Specifically, the hybrid method, combining the high-dynamic-range acceleration measurement with the spatially dense high-speed-camera measurement, proposed by Javh *et al.* [20], was used to identify modes even where the noise floor was above the usable signal. With the hybrid method, the high-dynamic ćrange accelerometer measurement is used to identify the complex poles of the structure (LSCF method):

$${}_{\mathrm{acc}}\lambda_r = -\zeta_r\,\omega_r \pm \mathrm{i}\,\omega_r\,\sqrt{1-\zeta_r^2}. \tag{2}$$

The low dynamic range, high spatial density data from the high-speed camera are then combined with the identified poles to identify the high spatial density modal shapes (LSFD method). The LSCF and LSFD methods are implemented in the open-source Python package pyEMA [21].

## 2.3 Finite element model updating - sensitivity based methods

To identify the parameters, $\boldsymbol{\theta}$, of a finite element model with the sensitivity-based (sometimes called iterative) methods, the measured data, $\mathbf{z}_{\mathrm{m}}$, is compared with the data obtained from the numerical simulation in the $j$-th iteration, $\mathbf{z}_j$. The data vectors $\boldsymbol{z}_{\mathrm{m}}$ and $\boldsymbol{z}_j$ usually contain the natural frequencies and modal shapes. In each iteration $j$, new approximations of the unknown parameters, $\boldsymbol{\theta}_{j+1}$, are computed:

$$\boldsymbol{\theta}_{j+1} = \boldsymbol{\theta}_j + \left[\mathbf{S}_j^T \cdot \mathbf{W}_{\varepsilon\varepsilon} \cdot \mathbf{S}_j + \mathbf{W}_{\theta\theta}\right]^{-1} \cdot \mathbf{S}_j^T \cdot \mathbf{W}_{\varepsilon\varepsilon} \cdot \big(\mathbf{z}_{\mathrm{m}} - \mathbf{z}_j\big), \tag{3}$$

where $\mathbf{W}_{\varepsilon\varepsilon}$ is a diagonal matrix with reciprocal values of the variances of the measured data, $\mathbf{W}_{\theta\theta}$ is a diagonal matrix with reciprocal values of the estimated variances of the parameters and $\boldsymbol{S}_j$ is the sensitivity matrix in the $j$-th iteration. When the number of updating parameters $m$ is larger than the number of residuals $n$, the updating parameters cannot be uniquely identified. The Tikhonov regularization [22] is used to obtain the solution with the minimal change in updating parameters. In this research, noisy measurements are used and location-specific weighting of the modal shapes is introduced by Eq. (3). All of the parameters were given equal weight in $\mathbf{W}_{\theta\theta}$, chosen so that the Euclidean norm of $\mathbf{W}_{\theta\theta}$ was equal to the Euclidean norm of $\mathbf{W}_{\varepsilon\varepsilon}$.

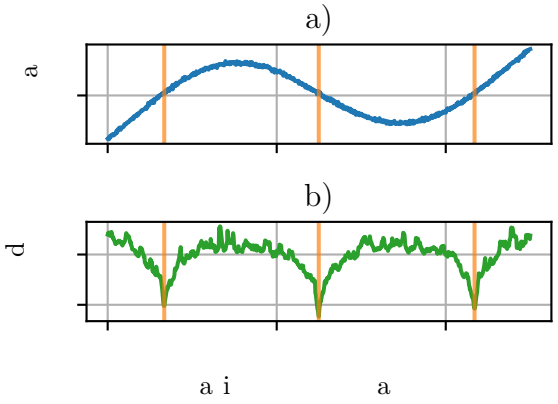


Figure 1: a) normalized modal shape from dataset B and b) local Signal-to-Noise Ratio along the beam. A moving average with a kernel size of 10 was used to compute the local SNR.

## 3 Location-specific weighting of noisy data

Eq. (3) enables weighting of individual elements of vector $\boldsymbol{z}_{\mathrm{m}}$, the location-specific weighting of the modal shapes was investigated. The basis for the location weighing is the fact that the SNR is not constant for the whole modal shape; rather it is very low in the nodal Degrees Of Freedom (DOFs) and larger in the areas with large deformation. The local SNR is shown in Fig. 1.

Three methods of modal shape weighting were compared in this research: unitary weighting, absolute weighting and square weighting. With the unitary weighting, all locations were given equal weight, not taking into account the low SNR at nodal DOFs:

$$w_{\varepsilon,\phi_i,j} = w, \qquad j = 1 \dots n_{\text{locations}} \tag{4}$$

With the absolute weighting, each location was weighted with the absolute value of the modal shape itself, see Eq. (5), giving lower weight to the nodal DOFs.

$$w_{\varepsilon,\phi_i,j} = \frac{|\phi_{i,j}|}{\sqrt{\sum_{i=1}^{n_{\text{modes}}} \sum_{k=1}^{n_{\text{locations}}} \phi_{i,k}^2}}, \qquad j = 1 \dots n_{\text{locations}}. \tag{5}$$

The difference in weighting of the nodal DOFs and the DOFs with large deformation was increased by using the square weighting, where the square of the modal shape was used as a weight:

$$w_{\varepsilon,\phi_i,j} = \frac{\phi_{i,j}^2}{\sqrt{\sum_{i=1}^{n_{\text{modes}}} \sum_{k=1}^{n_{\text{locations}}} \phi_{i,k}^2}}, \qquad j = 1 \dots n_{\text{locations}} \tag{6}$$

The weights for all the eigenvalues and modal shapes were assembled in a diagonal weighting matrix:

$$\mathbf{W}_{\varepsilon\varepsilon} = \text{diag}(w_{\varepsilon,\lambda_0}, w_{\varepsilon,\lambda_1}, ..., \mathbf{w}_{\varepsilon,\phi_0}^T, \mathbf{w}_{\varepsilon,\phi_1}^T, ...) \tag{7}$$

where $w_{\varepsilon,\lambda_i}$ is the weight of eigenvalue $\lambda_i$ and $\mathbf{w}_{\varepsilon,\phi_i}$ is the vector weight of modal shape $\boldsymbol{\phi}_i$, computed with Eq. (4), (5) or (6). The weight of eigenvalues $w_{\varepsilon,\lambda_i}$ were chosen as a Euclidean norm of $\boldsymbol{\phi}_i$, giving $\lambda_i$ and $\boldsymbol{\phi}_i$ equal weight.

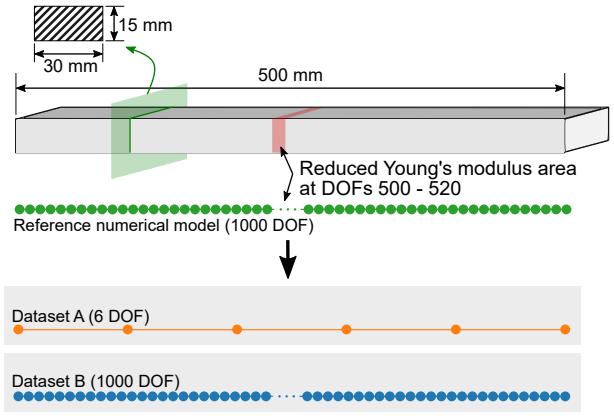


Figure 2: Beam dimensions in the reference numerical model. Translational degrees of freedom for dataset A and dataset B are presented.

## 4 Numerical case study

The research was carried out on the simulated data, where the real values of the model parameters are known, enabling the direct comparison with the updated parameters. The measurement was simulated using the reference numerical model, created by modeling a beam (Fig. 2) with 999 Euler-Bernoulli finite elements [23]. The density of the material, $\rho$, for the reference model was 7400 kg/m$^3$ and the Young's modulus, $E$, was 180 GPa. To introduce a parameter variation, the Young's modulus was reduced (36 GPa) for elements at locations from 500 through 520. A free-free boundary condition was applied and no damping was included.

From the reference numerical model, two reference datasets with the first five eigenvalues and the associated modal shapes (excluding rigid-body modes) were extracted, *i.e.*, reference datasets A and B (Fig. 2). The modal shapes in dataset A were generated in 6 translational Degrees Of Freedom (DOFs), to simulate the spatially sparse accelerometer measurement. Modal shapes in dataset B were generated in 1000 translational DOFs, simulating the spatially dense high-speed-camera measurement. The rotational DOFs were excluded from the modal shapes. Normally distributed noise was added to the modal shapes of both datasets:

$$\hat{\boldsymbol{\phi}} = \mathbf{S} + \mathbf{N}, \tag{8}$$

where $\hat{\boldsymbol{\phi}}$ is the modal shape contaminated with noise, $\mathbf{S}$ is the modal shape without noise and $\mathbf{N}$ is the zero-mean noise signal, which was generated to obtain the desired Signal-to-Noise Ratio (SNR). Tab. 1 shows the SNRs used for the different modal shapes and datasets (dataset A was given a higher SNR than dataset B).

Table 1: Modal shape SNR [dB] for datasets A and B.

| Mode nr. | A (6 DOF) | B (1000 DOF) |
|---|---|---|
| 1 | 70 | 30 |
| 2 | 67 | 27 |
| 3 | 64 | 24 |
| 4 | 61 | 21 |
| 5 | 58 | 18 |

The finite-element model was updated using the sensitivity approach, see Sec. 2.3, and the Young's moduli of all the elements were chosen as the updating parameters. In the updating procedure, the eigenvalue and modal-shape residuals were minimized. The eigenvalue residuals were computed as:

$$z_{\lambda,i} = \frac{\lambda_i - \hat{\lambda}_i}{\hat{\lambda}_i} \tag{9}$$

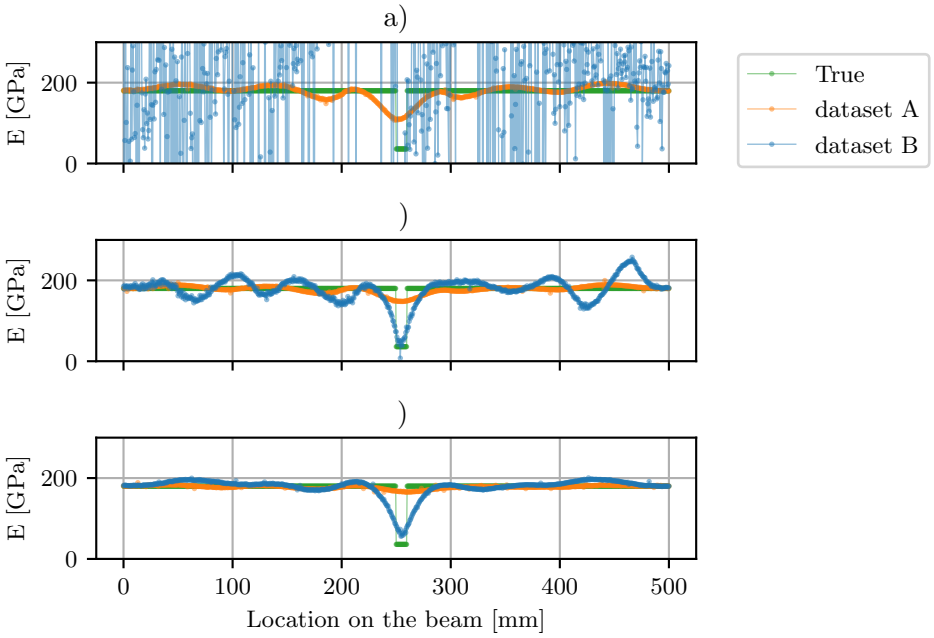


Figure 3: Young modulus along the beam as a result of different weighting methods. a) unitary, b) absolute and c) square weighting.

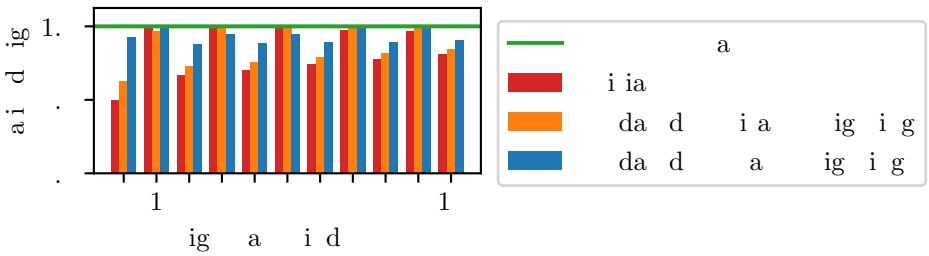


Figure 4: Comparison of normalized eigenvalues before and after updating with unitary weighting (dataset A) and square weighting (dataset B).

where $\lambda_i$ is the $i$-th numerical eigenvalue and $\hat{\lambda}_i$ is the corresponding eigenvalue from the reference dataset. The modal-shapes residuals were computed location-by-location:

$$z_{\phi,i,j} = \frac{\phi_{i,j} - \hat{\phi}_{i,j}}{\sqrt{\sum_{i=1}^{n_{\text{modes}}} \sum_{k=1}^{n_{\text{locations}}} \hat{\phi}_{i,k}^2}}, \qquad j = 1 \ldots n_{\text{locations}} \tag{10}$$

Each of the three weighting methods were used to update the finite-element model. The results in Fig. 3 show that the unitary weighting is not appropriate for the low-dynamic-range data in dataset B, since the updated Young's moduli are far from physically meaningful. For dataset A, the unitary weighting performs best; however, for dataset B, the best agreement between the updated and true values of the Young's moduli was achieved using the square weighting, see Fig. 3c.

The updated eigenvalues, normalized to the reference values, for the best-performing weighting (dataset A with unitary weighting and dataset B with square weighting), are compared in Fig. 4. It is clear that the updated eigenvalues, along with the ones not included in the updating process, are closer to the reference values when dataset B was used, even with the lower SNR of the modal shapes.

## 5 Conclusions

This study researches different types of modal shape weighting in the finite element model updating procedure. The location-specific weights were chosen based on the fact that the SNR is not constant throughout the structure, but is low at the nodal locations. The unitary, absolute and square weighting methods were researched on the numerical experiment, where the true values of the parameters are known. It was found, that for the high-spatial density modal shapes with large noise amplitude applied (low SNR), the square weighting produces the best results. For the low-spatial density modal shapes with high SNR, the unitary weighting was found to produce better results. This research shows, that for model updating with the modal data obtained from the high-speed camera, the square weighting should be used to improve the identification of the finite-element model parameters.

## References

[1] M. Friswell and J. E. Mottershead, *Finite element model updating in structural dynamics*. Springer Science & Business Media, 2013, vol. 38.

[2] H. Zhu, J. Li, W. Tian, S. Weng, Y. Peng, Z. Zhang, and Z. Chen, "An enhanced substructure-based response sensitivity method for finite element model updating of large-scale structures," *Mechanical Systems and Signal Processing*, vol. 154, p. 107359, 2021.

[3] M. Rezaiee-Pajand, A. Entezami, and H. Sarmadi, "A sensitivity-based finite element model updating based on unconstrained optimization problem and regularized solution methods," *Structural Control and Health Monitoring*, vol. 27, no. 5, pp. 1–29, 2020.

[4] M. Girardi, C. Padovani, D. Pellegrini, and L. Robol, "A finite element model updating method based on global optimization," *Mechanical Systems and Signal Processing*, vol. 152, p. 107372, 2021.

[5] H.-P. Wan and W.-X. Ren, "Parameter Selection in Finite-Element-Model Updating by Global Sensitivity Analysis Using Gaussian Process Metamodel," *Journal of Structural Engineering*, vol. 141, no. 6, p. 04014164, 2015.

[6] B. D. Lucas and T. Kanade, "An Iterative Image Registration Technique with an Application to Stereo Vision," in *Proceedings of the 7th International Joint Conference on Artificial Intelligence - Volume 2*, ser. IJCAI'81. San Francisco, CA, USA: Morgan Kaufmann Publishers Inc., 1981, pp. 674–679.

[7] W. H. Peters and W. F. Ranson, "Digital Imaging Techniques In Experimental Stress Analysis," *Optical Engineering*, vol. 21, no. 3, p. 213427, jun 1982.

[8] M. N. Helfrick, C. Niezrecki, P. Avitabile, and T. Schmidt, "3D digital image correlation methods for full-field vibration measurement," *Mechanical Systems and Signal Processing*, vol. 25, no. 3, pp. 917–927, 2011.

[9] D. Gorjup, J. Slavič, and M. Boltežar, "Frequency domain triangulation for full-field 3D operating-deflection-shape identification," *Mechanical Systems and Signal Processing*, vol. 133, 2019.

[10] C. Yang, "An adaptive sensor placement algorithm for structural health monitoring based on multi-objective iterative optimization using weight factor updating," *Mechanical Systems and Signal Processing*, vol. 151, p. 107363, 2021.

[11] W. Wang, J. E. Mottershead, A. Ihle, T. Siebert, and H. Reinhard Schubach, "Finite element model updating from full-field vibration measurement using digital image correlation," *Journal of Sound and Vibration*, vol. 330, no. 8, pp. 1599–1620, apr 2011.

[12] J. W. Ngan, C. C. Caprani, and Y. Bai, "Full-field finite element model updating using Zernike moment descriptors for structures exhibiting localized mode shapes," *Mechanical Systems and Signal Processing*, vol. 121, pp. 373–388, 2019.

[13] A. Zanarini, "Full field optical measurements in experimental modal analysis and model updating," *Journal of Sound and Vibration*, vol. 442, pp. 817–842, 2019.

[14] D. P. Rohe, "Using high-resolution measurements to update finite element substructure models," in *Rotating Machinery, Vibro-Acoustics & Laser Vibrometry, Volume 7*. Springer, 2019, pp. 137–148.

[15] M. Cuadrado, J. Pernas-Sánchez, J. Artero-Guerrero, and D. Varas, "Model updating of uncertain parameters of carbon epoxy composite plates using digital image correlation for full-field vibration measurement," *Measurement*, vol. 159, p. 107783, 2020.

[16] K. Zaletelj, J. Slavič, and M. Boltežar, "Full-field dic-based model updating for localized parameter identification," *Mechanical Systems and Signal Processing*, vol. 164, p. 108287, 2022.

[17] P. Guillaume, L. Hermans, and H. Van der Auweraer, "Maximum Likelihood Identification of Modal Parameters from Operational Data," *Proceedings of the 17th International Modal Analysis Conference (IMAC17)*, pp. 1887–1893, 1999.

[18] H. Van der Auweraer, W. Leurs, P. Mas, and L. Hermans, "Modal parameter estimation from inconsistent data sets," in *Proceedings of SPIE-The International Society for Optical Engineering*, vol. 4062, 2000.

[19] B. Cauberghe, "Applied frequency-domain system identification in the field of experimental and operational modal analysis," Ph.D. dissertation, Vrije Universiteit Brussel, 2004.

[20] J. Javh, J. Slavič, and M. Boltežar, "High frequency modal identification on noisy high-speed camera data," *Mechanical Systems and Signal Processing*, vol. 98, pp. 344–351, 2018.

[21] K. Zaletelj, T. Bregar, D. Gorjup, and J. Slavič, "ladisk/pyema: v0.24," Sep. 2020.

[22] A. N. Tikhonov, "On the solution of ill-posed problems and the method of regularization," in *Doklady Akademii Nauk*, vol. 151, no. 3. Russian Academy of Sciences, 1963, pp. 501–504.

[23] O. Bauchau and J. Craig, "Euler-Bernoulli beam theory," in *Structural analysis*. Springer, 2009, pp. 173–221.